References

[1] R. G. Veltrop and R. B. Wilds, "Modified tables for the design of optimum diplexers," *Microwave J.*, vol. 7, pp. 76–80, June 1964.

[2] R. J. Wenzel, "Application of exact synthesis methods to multichannel filter design," *IEEE Trans. Microwave Theory and Techniques*, vol. MTT-13, pp. 5–15, January 1965.

[3] G. L. Matthaei and E. G. Cristal, "Multiplexer channel-separating units using interdigital and parallel-coupled filters," *IEEE Trans. Microwave Theory and Techniques*, vol. MTT-13, pp. 328–334, May 1965.

[4] G. L. Matthaei, L. Young, and E. M. T. Jones, *Microwave Filters, Impedance Matching Networks and Coupled Structures.* New York: McGraw-Hill, 1964.

[5] M. C. Horton and R. J. Wenzel, "Realization of microwave filters with equal ripple response in both pass and stop bands" in *Proceedings of the Symposium on Generalized Networks*, vol. 16. Brooklyn, N. Y.: Polytechnic Institute of Brooklyn Press, 1966, pp. 257–287.

[6] R. J. Wenzel and M. C. Horton, "Design techniques for TEM networks," USAEL Contract DA28-043 AMC-01869(E), Semi-Annual Rept., August 1966.

[7] M. C. Horton and R. J. Wenzel, "The digital elliptic filter—a compact sharp-cutoff design for wide bandstop or bandpass requirements," *IEEE Trans. Microwave Theory and Techniques*, vol. MTT-15, pp. 307–314, May 1967.

[8] E. A. Guillemin, *Synthesis of Passive Networks.* New York: Wiley, 1957.

[9] L. Weinberg, *Network Analysis and Synthesis.* New York: McGraw-Hill, 1962.

[10] J. K. Skwirzynski, *Design Theory and Data for Electric Filters.* London: Van Nostrand, 1965.

[11] J. A. C. Bingham, "A new method of solving the accuracy problem in filter design," *IEEE Trans. Circuit Theory*, vol. CT-11, pp. 327–341, September 1964.

[12] T. Fujisawa, "Realizability theorem on mid-series or mid-shunt low-pass ladders without mutual induction," *IRE Trans. Circuit Theory*, vol. CT-2, pp. 320–325, December 1955.

[13] R. Saal and E. Ulbrich, "On the design of filters by synthesis," *IRE Trans. Circuit Theory*, vol. CT-5, pp. 284–327, December 1958.

[14] J. Meinguet and V. Belevitch, "On the realizability of ladder filters," *IRE Trans. Circuit Theory*, vol. CT-5, pp. 253–255, December 1958.

[15] R. Saal, "Der Entwurf von Filtern mit Hilfe des Kataloges normierter Tiefpässe" (in German), Telefunken, Backnang, Germany, 1961.

[16] W. J. Getsinger, "Coupled rectangular bars between parallel plates," *IRE Trans. Microwave Theory and Techniques*, vol. MTT-10, pp. 65–72, January 1962.

[17] *The Microwave Engineer's Handbook and Buyer's Guide.* Brookline, Mass.: Horizon House-Microwave, Inc., 1966, p. 91.

Radial Line Band Rejection Filters in Coaxial Waveguides

DAN VARON, MEMBER, IEEE

Abstract—**A coaxial waveguide with a cylindrical cavity forming a double discontinuity in the outer conductor is known to serve as a band rejection filter in the microwave region. A variational principle is applied to calculate the rejection frequency and a subsequent analysis is conducted to determine the dependence of that frequency on various parameters of the structure. Results are presented graphically and by simple analytical formulas. They demonstrate a newly discovered relationship between the rejection frequency and the width of the cavity, and provide design information which enables prediction of the rejection frequency within a 1 percent accuracy.**

Introduction

AMONG THE SIMPLEST and least expensive structures that serve as band rejection filters in the microwave region is the coaxial waveguide with a cylindrical cavity forming a discontinuity in the outer conductor (Fig. 1). The band rejection properties of such structures are exploited in multiple frequency circuits, such as parametric amplifiers,[1] where frequency separation has very stringent requirements. When the outer conductor of a coaxial waveguide is perturbed to form a cylindrical cavity, the TEM mode is totally reflected at a resonant frequency that depends on as many as six parameters. These are the inner and outer radii of the coaxial line, the radius and width of the cavity, and the dielectric constants of the cavity and the line. The rejection frequency is more sensitive to some parameters than to others. Experience indicates that in restricted regions certain approximate methods, in which the effects of one or several of the less sensitive parameters are neglected, provide remarkably accurate results. However, there are discrepancies of 5 percent or more in other regions where the same approximations ought to be valid.[1],[2] The approximations most frequently used by filter designers correspond to either one of the following situations: a) total disregard of the fringing fields caused by the two close discontinuities in which case the cylindrical cavity is viewed as a series impedance equal to the input impedance of a shorted radial transmission line;[3] or b) consideration of the fringing fields associated with each discontinuity but neglect of the interaction between the two. In the latter, the discontinuities are accounted for by equivalent shunt-lumped reactive elements; however, they must be far enough apart so that the interaction is indeed negligible. A common feature of both cases is that they neglect to consider the cavity width.

Manuscript received April 19, 1967; revised August 1, 1967. This work was supported by the U. S. Army under Contract DA-30-069-AMC-333(Y).

The author is with Bell Telephone Laboratories, Inc., Whippany, N. J.

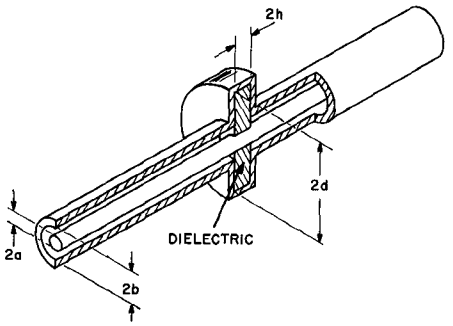

Fig. 1. Radial line coaxial filter.

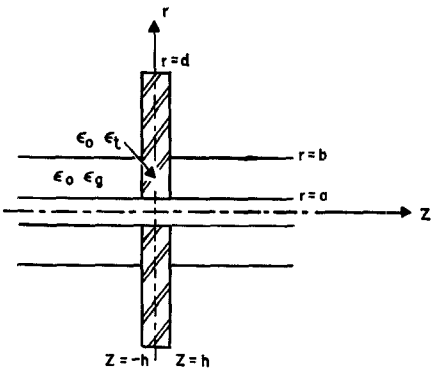

Fig. 2. Longitudinal cross section (inner dimensions).

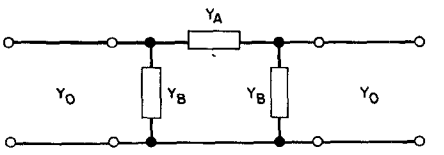

Fig. 3. Equivalent circuit for the TEM mode.

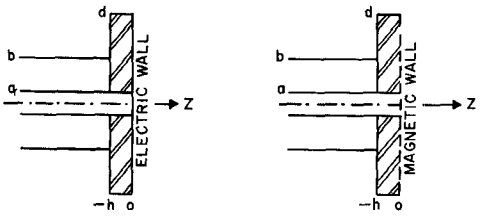

Fig. 4. (a) Short-circuit bisection. (b) Open-circuit bisection.

The following study is motivated by the objective of gaining further understanding of the relationship between the rejection frequency and the physical parameters of the structure, in particular the width of the cavity. This is accomplished by a solution which very accurately predicts the rejection frequency. This high accuracy is obtained by consideration of all six parameters mentioned. Only second-order effects such as losses in conductors and dielectrics are neglected.[1] As a result, new quantitative data are obtained over a very wide band in the microwave region where coaxial lines are practical.

The analysis includes a representation of the double discontinuity by a symmetric two-port,[4] whose admittance matrix Y is derived from a variational principle.[5] Through application of the Rayleigh-Ritz method,[6] the points of infinite insertion loss are computed by finding the zeros of the y_{12} element of Y.

The results are presented as families of curves, computed on a normalized basis, with the resonant wavelength in the cylindrical cavity as a natural unit of length. The same results are also given in terms of analytical formulas in various regions of the normalized parameters. The calculated results agree with experimental measurements within 1 percent.

Theoretical Analysis

Definitions

Let the structure be placed in a right-handed cylindrical coordinate system (Fig. 2) the origin of which coincides with the center of the cylindrical cavity, and whose axis coincides with that of the coaxial waveguide. The following notation is adopted for the physical parameters pertinent to the analysis:

a = inner radius of coaxial waveguide
b = outer radius of coaxial waveguide
d = outer radius of cavity
$2h$ = width of cavity
ϵ_0 = dielectric constant of air
ϵ_g = relative dielectric constant of the medium inside the coaxial waveguide ($a \leq r \leq b$, $z > |h|$)
ϵ_t = relative dielectric constant of the medium inside the cavity ($a \leq r \leq d$, $z \leq |h|$)
μ_0 = permeability of free space.

[1] Losses are essential in obtaining data on actual rejection. In a lossless structure the insertion loss is infinite at the rejection frequency.

The conducting walls are considered perfect, and the dielectric media are assumed to be lossless. The radii a and b are such that only the TEM mode can propagate in the coaxial line.

Formulation

The main interest in this problem is to find under what conditions the TEM mode will be totally reflected by the double discontinuity. The entire structure may be represented by an equivalent circuit to the TEM mode wherein the coaxial waveguide is represented by a uniform transmission line and the cylindrical cavity by a symmetric π network. That equivalent circuit is shown in Fig. 3. To find the two unknown admittances Y_A and Y_B, two linearly independent excitations, a symmetrical and an antisymmetrical one, are chosen. With those particular excitations the symmetry plane $z=0$ behaves like a magnetic wall for symmetrical excitation and like an electric wall for the antisymmetrical one. Consequently, the structure may be bisected at $z=0$ and terminated alternately by an open- and short-circuit boundary. Thus, the problem of the double discontinuity is reduced to two similar problems of a terminated coaxial waveguide with only one step discontinuity, as shown in Fig. 4. A field analysis in both cases yields variational expressions for the open- and short-circuit input admittances at $z=-h$, from which the resonance condition $Y_A(\omega)=0$ can be readily obtained.

Field Analysis

An incident TEM wave propagating in the positive z direction is partly reflected by the discontinuity and partly transmitted through the interface between the coaxial guide and the bisected cavity. The transmitted wave is totally reflected at $z=0$, thus forming a standing wave in the cavity. Also, the discontinuity gives rise to an infiite number of higher-order TM_{0n} modes in both regions. If a time harmonic dependence $e^{j\omega t}$ is assumed, the transverse components of the electromagnetic field are given as follows.

1) In the coaxial guide $(-\infty < z \leq -h)$

$$E_{r1}^{(i)}(r, z) = \frac{A_0^{(i)}}{r}\left[e^{-jk_1(z+h)} + R_i e^{jk_1(z+h)}\right] + \sum_{n=1}^{\infty} A_n^{(i)}\phi_n(r)e^{j\beta_n z} \tag{1}$$

$$H_{\theta 1}^{(i)}(r, z) = \frac{A_0^{(i)}}{\eta_1 r}\left[e^{-jk_1(z+h)} - R_i e^{jk_1(z+h)}\right] - \sum_{n=1}^{\infty} A_n^{(i)}\frac{k_1}{\eta_1\beta_n}\phi_n(r)e^{j\beta_n z} \quad i = 1, 2 \tag{2}$$

where $i=1$ is to be taken for the case of open-circuit bisection and $i=2$ for short-circuit bisection; R_i is the reflection coefficient of the TEM mode at the plane of the discontinuity, $k_1=\omega(\mu_0\epsilon_0\epsilon_g)^{1/2}$, $\eta_1=(\mu_0/\epsilon_0\epsilon_g)^{1/2}$

$$\phi_n(r) = J_0(\lambda_n a)Y_1(\lambda_n r) - Y_0(\lambda_n a)J_1(\lambda_n r) \qquad a \leq r \leq b \tag{3}$$

where $J_p(x)$ and $Y_p(x)$, $p=0, 1$, are the Bessel and Neumann functions of order p, and $\{\lambda_n\}$, $n=1, 2, \cdots, \infty$, are eigenvalues which satisfy

$$J_0(\lambda_n a)Y_0(\lambda_n b) - Y_0(\lambda_n a)J_0(\lambda_n b) = 0 \qquad n = 1, 2, \cdots, \infty. \tag{4}$$

β_n is determined by the dispersion relation

$$\lambda_n^2 + \beta_n^2 = k_1^2. \tag{5}$$

The aforementioned assumption that all higher-order modes in $z \leq -h$ are evanescent implies $\lambda_n > k_1$ and $\beta_n = -j|\beta_n|$, $n \geq 1$.

2) In the cavity $(-h \leq z \leq 0)$

$$E_{r2}^{(i)}(r, z) = \frac{B_0^{(i)}}{r}T_i(k_2 z) + \sum_{n=1}^{\infty} B_n^{(i)}\hat{\phi}_n(r)T_i(\kappa_n z) \tag{6}$$

$$H_{\theta 2}^{(i)}(r, z) = \frac{B_0^{(i)}}{\eta_2 r}T_{i+1}(k_2 z) + \sum_{n=1}^{\infty} B_n^{(i)}\frac{k_2}{\eta_2\kappa_n}\hat{\phi}_n(r)T_{i+1}(\kappa_n z) \quad i = 1, 2 \tag{7}$$

where

$$T_1(x) = T_3(x) = \cos x \tag{8a}$$

$$T_2(x) = -j \sin x \tag{8b}$$

and the choice of i is the same as the foregoing.

$$\hat{\phi}_n(r) = J_0(\sigma_n a)Y_1(\sigma_n r) - Y_0(\sigma_n a)J_1(\sigma_n r) \tag{9}$$

with $\{\sigma_n\}$ being a set of eigenvalues satisfying

$$J_0(\sigma_n a)Y_0(\sigma_n d) - Y_0(\sigma_n a)J_0(\sigma_n d) = 0 \qquad n = 1, 2, \cdots, \infty. \tag{10}$$

κ_n is given by the dispersion relation

$$\sigma_n^2 + \kappa_n^2 = k_2^2 \tag{11}$$

where $k_2=\omega(\mu_0\epsilon_0\epsilon_t)^{1/2}$ and $\eta_2=(\mu_0/\epsilon_0\epsilon_t)^{1/2}$.

The eigenfunctions $\{\phi_n(r)\}$ and $\{\hat{\phi}_n(r)\}$ satisfy the following orthogonality conditions:[7]

$$\int_a^b \phi_n(r)dr = \int_a^d \hat{\phi}_n(r)dr = 0 \quad n = 1, 2, \cdots, \infty \tag{12a}$$

$$\int_a^b \phi_n(r)\phi_m(r)rdr = N_n^2\delta_{nm} \quad n, m = 1, 2, \cdots, \infty \tag{12b}$$

$$\int_a^d \hat{\phi}_n(r)\hat{\phi}_m(r)rdr = S_n^2\delta_{nm} \quad n, m = 1, 2, \cdots, \infty \tag{12c}$$

where

$$N_n^2 = \frac{b^2}{2}\phi_n^2(b) - \frac{2}{\pi^2\lambda_n^2} \tag{13a}$$

$$S_n^2 = \frac{d^2}{2}\hat{\phi}_n^2(d) - \frac{2}{\pi^2\sigma_n^2} \tag{13b}$$

$$\delta_{nm} = \begin{cases} 1 & n = m \\ 0 & n \neq m. \end{cases} \tag{13c}$$

At the interface $z=-h$ the radial electric and circumferential magnetic field components satisfy the following continuity conditions:

$$E_{r1}^{(i)}(r, -h) = E_{r2}^{(i)}(r, -h) \qquad a \leq r < b \tag{14a}$$

$$H_{\theta 1}^{(i)}(r, -h) = H_{\theta 2}^{(i)}(r, -h) \qquad i = 1, 2 \tag{14b}$$

$$E_{r2}^{(i)}(r, -h) = 0 \qquad b \leq r \leq d. \tag{14c}$$

At this stage of the analysis the unknown quantities are R_i, $A_{n+1}^{(i)}$, and $B_n^{(i)}$, $i=1, 2$; $n=0, 1, 2 \cdots, \infty$, whereas $A_0^{(i)}$ is an arbitrary normalization constant. By using the orthogonality property of the eigenfunctions $\phi_n(r)$ and $\hat{\phi}_n(r)$, all unknown constants may be written in terms of the aperture field $E_{r2}^{(i)}(r, -h)$, which henceforth will be denoted simply by $E_i(r)$. Also, whenever the index i appears it will be understood that $i=1, 2$.

Integrating (1) at $z=-h$ and using (12a) gives

$$A_0^{(i)}(1 + R_i) = \frac{1}{\ln\left(\frac{b}{a}\right)}\int_a^b E_i(r)dr. \tag{15}$$

Multiplying (1) by $r\phi_m(r)dr$ and integrating yields

$$A_m^{(i)}e^{-j\beta_m h} = \frac{1}{N_m^2}\int_a^b E_i(r)\phi_m(r)rdr \qquad m = 1, 2, \cdots, \infty. \tag{16}$$

Similarly, from (6) and (14a) the coefficients $B_m^{(i)}$ are found to be

$$B_0^{(i)}T_i(-k_2h) = \frac{1}{\ln\left(\frac{d}{a}\right)}\int_a^b E_i(r)dr \tag{17}$$

$$B_m^{(i)}T_i(-\kappa_m h) = \frac{1}{S_m^2}\int_a^b E_i(r)\hat{\phi}_m(r)rdr \qquad m = 1, 2, \cdots, \infty. \tag{18}$$

The integrations on the right-hand side of (17) and (18) are carried only from a to b, since $E_i(r)=0$, $b\leq r\leq d$. Substitution of (15) through (18) into (14b), via (2) and (7) gives

$$y_i\int_a^b E_i(r')dr' = \int_a^b K_i(r\,|\,r')E_i(r')dr' \tag{19}$$

where

$$K_i(r\,|\,r') = \ln\left(\frac{b}{a}\right)\left\{\left(\frac{\epsilon_t}{\epsilon_g}\right)^{1/2}\frac{T_{i+1}(-k_2h)}{T_i(-k_2h)\ln\left(\frac{d}{a}\right)} + k_1rr'\sum_{n=1}^{\infty}\left[\frac{\epsilon_t}{\epsilon_g}\frac{T_{i+1}(-\kappa_n h)}{\kappa_n S_n^2 T_i(-\kappa_n h)}\hat{\phi}_n(r)\hat{\phi}_n(r') + \frac{1}{\beta_n N_n^2}\phi_n(r)\phi_n(r')\right]\right\} \tag{20}$$

$$y_i = \frac{1-R_i}{1+R_i}. \tag{21}$$

The constant y_i is recognizable as the normalized input admittance into the bisected cavity at the plane of discontinuity. Thus, y_1 is the normalized open-circuit bisection admittance, and y_2 is the normalized short-circuit bisection admittance. Kernel $K_i(r\,|\,r')$ is symmetric and purely imaginary. Constant $j(=\sqrt{-1})$ appears implicitly in (20). This may be verified by returning to (8) and to the paragraph between (5) and (6). Hence, y_i is reactive.

Equation (19) is an integral equation in which the unknown function is the aperture field $E_i(r)$, and the input admittance y_i is its characteristic value. A variational principle for y_i is obtained by multiplying the integral equation on both sides by $E_i(r)dr$ and integrating from a to b[8]

$$y_i = \frac{\int_a^b\int_a^b E_i(r)K_i(r\,|\,r')E_i(r')dr'dr}{\left[\int_a^b E_i(r)dr\right]^2}. \tag{22}$$

For the true value of $E_i(r)$ the absolute value of y_i is minimum and stationary. That is to say that an approximation to first order in $E_i(r)$ gives an approximation to second order in y_i.

A natural choice of a minimizing sequence[9] for $E_i(r)$ is its truncated modal expansion. Let

$$E_N^{(i)}(r) = \frac{a_0^{(i)}}{r} + \sum_{n=1}^{N} a_n^{(i)}\phi_n(r) \quad N \geq 1 \tag{23}$$

where $\{\phi_n(r)\}$ is a complete orthogonal set defined by (3) and (4). Denote by $y_N^{(i)}$ the value obtained by substituting $E_N^{(i)}(r)$ for $E_i(r)$ in (22). By the Rayleigh-Ritz method[6] if the amplitude coefficients $a_n^{(i)}$ are chosen so as to yield a minimum value of $|y_N^{(i)}|$ for every N, then when $N\to\infty$, $E_N^{(i)}(r)$ approaches the true aperture field $E_i(r)$ and $y_N^{(i)}$ approaches the true input admittance y_i. The coefficient $a_0^{(i)}$ may be chosen as an arbitrary normalization constant. Substitution of (23) into (22) yields

$$y_N^{(i)} = \frac{\sum_{s=0}^{N}\sum_{p=0}^{N} a_s^{(i)}a_p^{(i)}Q_{sp}^{(i)}}{[a_0^{(i)}]^2\ln\left(\frac{b}{a}\right)} \tag{24}$$

where

$$Q_{0p}^{(i)} = Q_{p0}^{(i)} = \sqrt{\frac{\epsilon_t}{\epsilon_g}}\frac{\left[\ln\left(\frac{b}{a}\right)\right]^2}{\ln\left(\frac{d}{a}\right)}\frac{T_{i+1}(-k_2h)}{T_i(-k_2h)}\delta_{0p} + k_1\left(\frac{\epsilon_t}{\epsilon_g}\right)\sum_{n=1}^{\infty}\frac{T_{i+1}(-\kappa_n h)}{T_i(-\kappa_n h)}\frac{P_n M_{np}^2}{\kappa_n S_n^2} \qquad p = 0, 1, 2, \cdots N, \tag{25a}$$

$$Q_{sp}^{(i)} = Q_{ps}^{(i)} = k_1\left[\frac{N_p^2}{\beta_p}\delta_{sp} + \frac{\epsilon_t}{\epsilon_g}\sum_{n=1}^{\infty}\frac{T_{i+1}(-\kappa_n h)}{T_i(-\kappa_n h)}\frac{M_{ns}^2 M_{np}^2}{\kappa_n S_n^2}\right] \qquad s, p = 1, 2, \cdots, N \tag{25b}$$

with

$$P_n = \int_a^b \hat{\phi}_n(r)dr = \frac{1}{\sigma_n}[Y_0(\sigma_n a)J_0(\sigma_n b) - J_0(\sigma_n a)Y_0(\sigma_n b)] \qquad n = 1, 2, \cdots, \infty \tag{26}$$

$$M_{np}^2 = \int_a^b r\hat{\phi}_n(r)\phi_p(r)dr = \frac{P_n b\phi_p(b)}{1-\left(\frac{\lambda_p}{\sigma_n}\right)^2} \qquad n = 1, 2, \cdots, \infty, \quad p = 1, 2, \cdots, N \tag{27a}[2]$$

$$M_{n0}^2 = P_n \quad n = 1, 2, \cdots, \infty \tag{27b}$$

$$\delta_{sp} = \begin{cases} 1 & s = p \\ 0 & s \neq p. \end{cases} \tag{28}$$

To minimize $|y_N^{(i)}|$ consider $y_N^{(i)}$ as a function of $N+1$ variables by rewriting (24) as

$$y_N^{(i)} = \frac{f[a_0^{(i)}, \cdots, a_N^{(i)}]}{g[a_0^{(i)}]}. \tag{29}$$

The minimizing coefficients satisfy the following set of $N+1$ equations

$$\frac{\partial y_N^{(i)}}{\partial a_p^{(i)}} = 0 \qquad p = 0, 1, \cdots, N. \tag{30}$$

[2] See G. N. Watson.[7]

That set can be reduced to $N+1$ linear algebraic equations by carrying out partial differentiations on (29) and letting the numerator vanish

$$\frac{\partial f}{\partial a_p^{(i)}} g - \frac{\partial g}{\partial a_p^{(i)}} f = 0 \qquad p = 0, 1, \cdots, N. \quad (31)$$

Dividing through by $2ga_0^{(i)}$ and noting that $\partial g/\partial a_p^{(i)} = 0$ if $p>0$ one obtains

$$-\ln\left(\frac{b}{a}\right) y_N^{(i)} + \sum_{s=1}^{N} Q_{0s}^{(i)} \alpha_s^{(i)} = -Q_{00}^{(i)} \quad (32a)$$

$$\sum_{s=1}^{N} Q_{ps}^{(i)} \alpha_s^{(i)} = -Q_{0p}^{(i)} \qquad p = 1, 2, \cdots, N \quad (32b)$$

where

$$\alpha_s^{(i)} = \frac{a_s^{(i)}}{a_0^{(i)}} \qquad s = 1, 2, \cdots, N. \quad (32c)$$

In (32) $y_N^{(i)}$ is one of the unknowns and it can be expressed in closed form as

$$y_N^{(i)} = \frac{1}{\ln\left(\frac{b}{a}\right)} \frac{\det (Q_i)}{\det (Q_i^M)} \quad (33)$$

where

$$Q_i = \left\| Q_{sp}^{(i)} \right\| \qquad s, p = 0, 1, 2, \cdots, N$$

$$Q_i^M = \left\| Q_{sp}^{(i)} \right\| \qquad s, p = 1, 2, \cdots, N.$$

By proper choice of N the true input admittance y_i may be approximated by $y_N^{(i)}$ and the resonance condition obtained by equating

$$y_1(\omega) = y_2(\omega). \quad (34)$$

A comparison of calculated and measured data shows that choosing $N=5$ yields an accuracy within 1 percent. In view of the complexity of (34) a digital computer must be used to obtain quantitative data.

Discussion of the Results

As a consequence of the scaling property of the electromagnetic field, the numerical work to solve (34) can be carried out on a normalized basis by expressing all linear dimensions in terms of a natural unit of length. This results in considerable economy in computing and data presentation over a wide range of frequencies. The normalization factor chosen in Figs. 5 through 11 is the wavelength λ_r in the medium filling the cavity at the rejection frequency $f_r = (\lambda_r \sqrt{\mu_0 \epsilon_0 \epsilon_t})^{-1}$. Every point on the curves yields, by unnormalization, the dimensions of a filter which rejects that frequency whose corresponding wavelength inside the cavity is the unnormalizing factor. In each one of Figs. 5 through 9 the normalized length of the cavity $L=(d-b)/\lambda_r$ is plotted against the normalized outer radius of the coaxial line $B=b/\lambda_r$ for various values of the normalized half-width of the cavity $H=h/\lambda_r$. Each set of curves is plotted at constant characteristic impedance of the coaxial line

$$Z_0 = \frac{60}{\sqrt{\epsilon_g}} \ln\left(\frac{b}{a}\right). \quad (35)$$

Figs. 5 through 7 are for 50 ohm lines with air and polyethylene dielectrics; and Figs. 8 and 9 are for minimum loss lines[10] of 92.6 ohms.

It is interesting to compare the results with those obtained by Schelkunoff for the input admittance of a shorted radial transmission line.[3] In Fig. 10 the curve marked S is normalized to the wavelength at which the radial transmission line has zero input admittance. The curve is given by

$$J_1(2\pi B) Y_0(2\pi D) - J_0(2\pi D) Y_1(2\pi B) = 0 \quad (36)$$

where

$$D = L + B \quad (37)$$

and $J_p(x)$, $Y_p(x)$, $p=0, 1$, are the Bessel and Neumann functions of order p. The derivation of (36) totally neglects the fringing fields at the input edge. Plot S is independent of the characteristic impedance of the coaxial line and of the cavity width. Therefore, it can be assumed that this curve constitutes a good approximation for very small values of H for which the fringing fields due to the double discontinuity are negligible. The question that remains to be answered is how small is "very small." The answer is found in Fig. 10 by comparing curves for various values of H with S. It can be seen that for $H \leq 0.001$ the constant H curves approach S very closely. Hence, one may interpret S as an asymptotic curve for $H \to 0$. The fact that curves for larger values of H cross the asymptotic curve indicates that L is a double valued function of H at constant B. This is illustrated more clearly in Fig. 11. Even though values of $H \leq 0.001$ are too small for practical applications in the microwave region, the asymptotic curve has served occasionally as a rather successful predictor of the rejection frequency. This is explained by the crossover of the asymptote by the actual curves at values of H two orders of magnitude larger than those at which final approach to the asymptote occurs.

The calculated results may be given in restricted regions by simple formulas of the following general form:

$$L = \alpha_0 + \alpha_1 H - \alpha_2 B + \alpha_3 HB. \quad (38)$$

The coefficients $\{\alpha_j\}, j=0, \ldots, 3$, are given in Tables I through III. The values obtained from (38) are within 0.5 percent of those obtained by the variational method if strict adherence to the specified regions is observed.

The rejection frequency calculated by the variational method agrees within 1 percent with experimental measurements by DeLoach, Jr.,[1] and also with those performed by this author. The latter are summarized in Table IV.

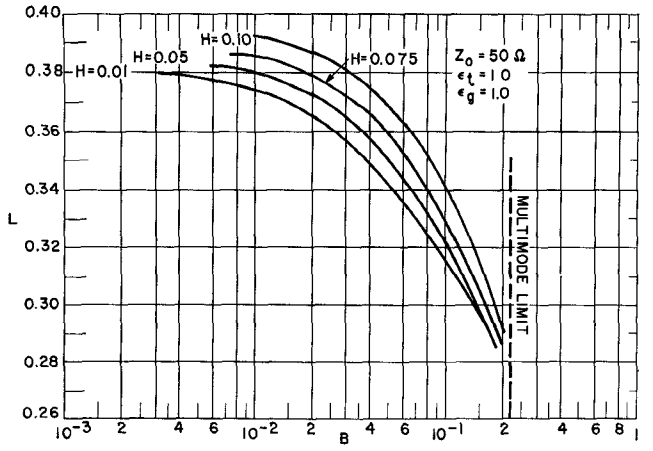

Fig. 5. Normalized cavity length versus normalized outer radius of coax for 50 ohm line air filled.

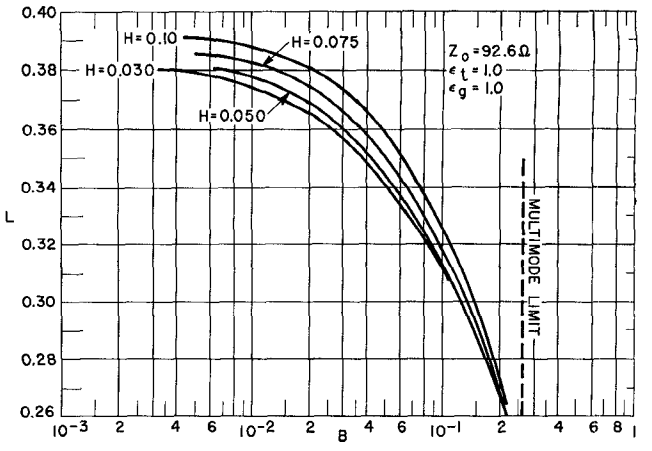

Fig. 8. Normalized cavity length versus normalized outer radius of coax for 92.6 ohm line air filled.

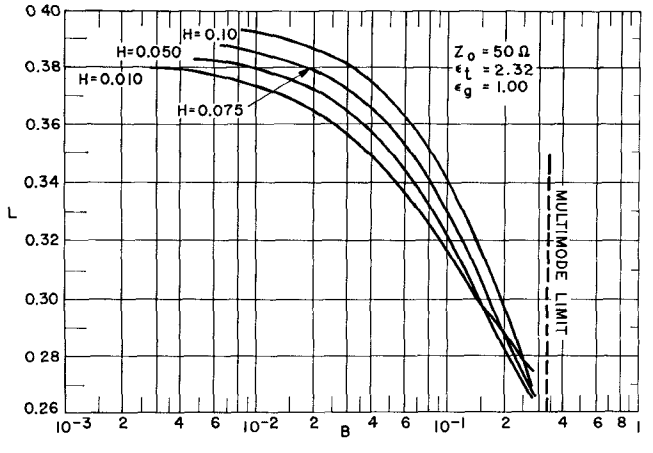

Fig. 6. Normalized cavity length versus normalized outer radius of coax for 50 ohm line air-filled coax and polyethylene-filled cavity.

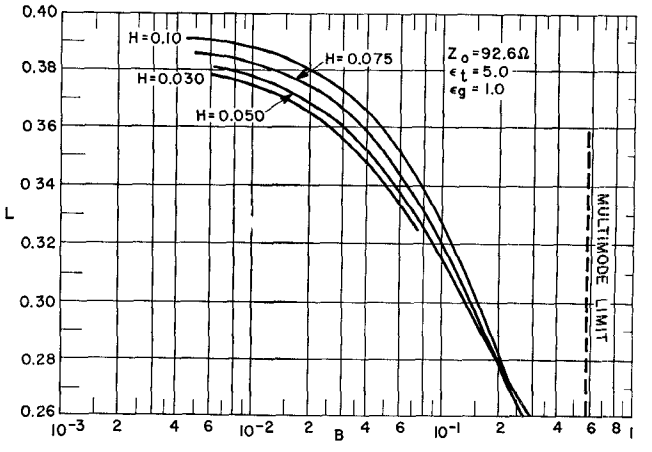

Fig. 9. Normalized cavity length versus normalized outer radius of coax for 92.6 ohm line air-filled coax and dielectric-filled cavity.

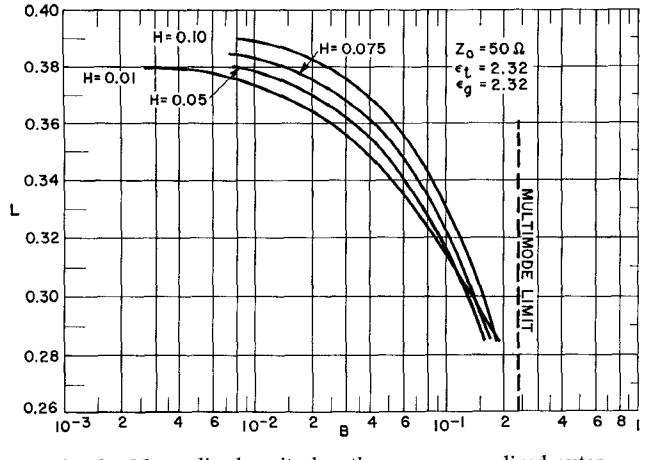

Fig. 7. Normalized cavity length versus normalized outer radius of coax for 50 ohm line polyethylene filled.

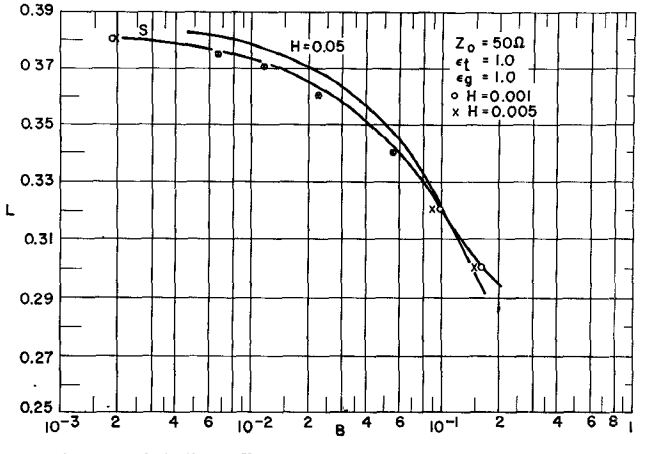

Fig. 10. Schelkunoff's curve S. The asymptote for $H \rightarrow 0$.

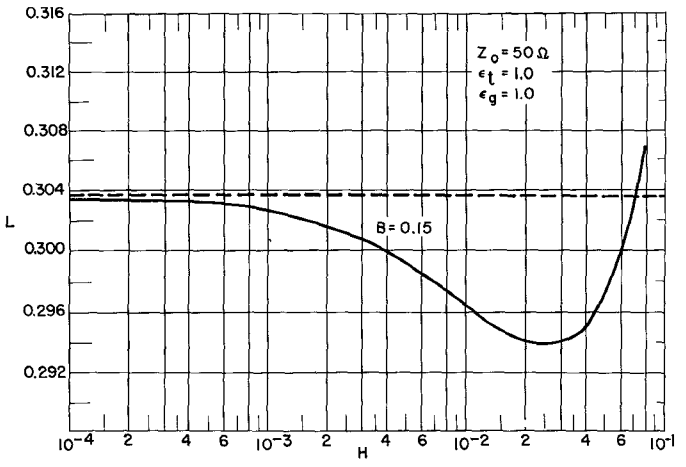

Fig. 11. Normalized cavity length versus normalized half-width of cavity.

TABLE I

$Z_0 = 50$ ohms, $\epsilon_g = 1.00$

ϵ_t	R_H*	R_B†	α_0	α_1	α_2	α_3
1.00	I	II	0.363	0.356	0.564	−0.952
1.00	I	III	0.343	0.412	0.364	−1.577
1.00	II	I	0.375	0.219	0.879	3.108
1.00	II	II	0.365	0.322	0.659	0.901
1.00	II	III	0.343	0.429	0.432	−0.329
2.32	I	II	0.361	0.384	0.520	−1.480
2.32	I	III	0.338	0.439	0.306	−1.970
2.32	II	I	0.375	0.220	0.872	3.051
2.32	II	II	0.364	0.329	0.632	0.719
2.32	II	III	0.336	0.482	0.363	−0.874
5.00	I	II	0.359	0.407	0.486	−1.881
5.00	I	III	0.336	0.447	0.269	−2.160
5.00	II	I	0.375	0.221	0.868	2.949
5.00	II	II	0.363	0.335	0.611	0.579
5.00	II	III	0.335	0.464	0.342	−0.810

* R_H: I $-0.03 \leq H \leq 0.05$
II $-0.05 \leq H \leq 0.10$
† R_B: I $-0.01 \leq B \leq 0.05$
II $-0.05 \leq B \leq 0.10$
III $-0.10 \leq B \leq 0.20$; $L \geq 0.290$

TABLE II

$Z_0 = 50$ ohms, $\epsilon_g = 2.32$

ϵ_t	R_H*	R_B†	α_0	α_1	α_2	α_3
2.32	I	I	0.379	0.145	0.849	1.463
2.32	I	II	0.362	0.280	0.564	−1.085
2.32	II	I	0.376	0.203	0.884	2.166
2.32	II	II	0.361	0.319	0.624	−0.014
2.32	II	III	0.342	0.387	0.437	−0.843

* R_H: I $-0.03 \leq H \leq 0.05$
II $-0.05 \leq H \leq 0.10$
† R_B: I $-0.005 \leq B \leq 0.06$
II $-0.06 \leq B \leq 0.11$
III $-0.11 \leq B \leq 0.185$; $L \geq 0.285$

TABLE III

$Z_0 = 92.6$ ohms, $\epsilon_g = 1.00$

ϵ_t	R_H*	R_B†	α_0	α_1	α_2	α_3
1.00	I	I	0.378	0.126	0.873	1.297
1.00	II	I	0.374	0.216	0.805	0.962
1.00	II	II	0.344	0.407	0.450	−1.423
5.00	I	I	0.377	0.150	0.799	0.101
5.00	II	I	0.374	0.201	0.822	1.320
5.00	II	II	0.344	0.375	0.408	−1.397

* R_H: I $-0.03 \leq H < 0.05$
II $-0.05 \leq H \leq 0.10$
† R_B: I $-0.005 \leq B \leq 0.070$
II $-0.070 \leq B \leq 0.150$

TABLE IV

$\epsilon_g = 1.00$, $\epsilon_t = 1.00$

$2a$ (inch)	$2b$ (inch)	$2d$ (inch)	$2h$ (inch)	f_c* (GHz)	f_m† (GHz)	$(f_m - f_c)/f_m$ (percent)
0.217	0.500	6.000	0.772	1.557	1.557	0.00
0.217	0.500	6.000	1.455	1.623	1.622	0.06
0.869	2.000	6.000	1.196	1.829	1.828	−0.05
0.869	2.000	6.000	0.054	1.770	1.767	−0.17
0.869	2.000	6.000	0.802	1.770	1.771	0.06
0.087	0.200	8.000	2.017	1.185	1.186	0.08
0.087	0.200	8.000	0.322	1.133	1.136	0.26
0.869	2.000	6.590	0.724	1.563	1.563	0.00
0.869	2.000	7.749	0.724	1.284	1.285	0.08

* Calculated resonant frequency.
† Measured resonant frequency.

Summary and Conclusions

The resonant frequency of a microwave radial line band rejection filter in a coaxial waveguide has been calculated by a variational method. The dependence of the resonant frequency on the physical parameters of the structure has been investigated and presented both graphically and analytically. It has been shown that the resonant frequency calculated by viewing the cylindrical cavity as a shorted radial transmission line is asymptotic to the true frequency when the cavity width is infinitesimally small with respect to the wavelength. Further, an explanation has been given why good results are obtained under certain conditions when total neglect of the fringing fields is not justified. A comparison of calculated results with experimental measurements shows agreement within 1 percent.

Acknowledgment

The author wishes to thank W. W. Mumford for bringing this problem to his attention, and for many inspiring discussions concerning the subject. The author also wishes to thank K. L. Steigerwalt for his kind assistance in performing the measurements.

References

[1] B. C. DeLoach, Jr., "Radial-line coaxial filters in the microwave region," *IEEE Trans. Microwave Theory and Techniques*, vol. MTT-11, pp. 50–55, January 1963.

[2] J. R. Whinnery, H. W. Jamieson, and T. E. Robbins, "Coaxial-line discontinuities," *Proc. IRE*, vol. 32, pp. 695–709, November 1944.

[3] S. A. Schelkunoff, *Electromagnetic Waves*. Princeton, N. J.: Van Nostrand, 1943, sec. 8.6, pp. 267–272.

[4] N. Marcuvitz and J. Schwinger, "On the representation of electric and magnetic fields produced by currents and discontinuities in waveguides," *J. Appl. Phys.*, vol. 22, pp. 806–819, June 1951.

[5] R. E. Collin, *Field Theory of Guided Waves*. New York: McGraw-Hill, 1960, ch. 8.

[6] P. M. Morse and H. Feshbach, *Methods of Theoretical Physics*. New York: McGraw-Hill, 1953, sec. 9.4.

[7] G. N. Watson, *A Treatise on the Theory of Bessel Functions*. 2nd ed. London: Cambridge University Press, 1962, pp. 132–135, eqs. (2), (8), (11).

[8] L. Cairo and T. Kahan, *Variational Techniques in Electromagnetism*. Glasgow, Scotland: Blackie and Son, Ltd., 1965, ch. 4, sec. 2(a).

[9] J. M. Gelfand and S. V. Fomin, *Calculus of Variations*. Englewood Cliffs, N. J.: Prentice-Hall, 1963, ch. 8.

[10] G. L. Ragan, *Microwave Transmission Circuits*, M.I.T. Rad. Lab. Ser., vol. 9. New York: McGraw-Hill, 1948, pp. 146–147.

[11] H. Westphalen, "Koaxialleitungsfilter mit radialen Leitungen" (in German) *Archiv. Elect. Übertragung*, vol. 19, pp. 637–646, December 1965, and *Archiv. Elect. Übertragung*, vol. 21, pp. 52–60, January 1967. (These references were brought to the author's attention by H. Westphalen after this work had been completed.)

A Computer Designed, 720 to 1 Microwave Compression Filter

HARRY S. HEWITT, MEMBER, IEEE

Abstract—**Compression filters with bandwidths up to 1000 MHz have application in high-resolution radar systems and rapid-scan receiver systems. A technique is presented for realizing a microwave linear delay (quadratic phase) versus frequency compression filter with sufficient delay accuracy to make compression ratios of up to 1000 to 1 feasible.**

The dispersive element in the compression filter is a silver tape with its broad side placed perpendicularly between the ground planes (instead of parallel, as in conventional stripline). The tape is folded back and forth upon itself in such a way that substantial coupling takes place between adjacent turns of the tape. A computer program has been written to determine the dimensions of the tape to achieve a linear delay versus frequency characteristic.

A folded tape compression filter was constructed with a differential delay of 1.2 μs over a bandwidth of 600 MHz centered at 1350 MHz giving a compression factor of 720 to 1. This filter was constructed in four identical sections, each section of which had a differential delay of 0.3 μs over the same bandwidth as the complete filter. The entire filter (four sections) occupies a volume about 16 by 4 by 5 inches. Measurement data are presented which illustrate that the desired accurate delay characteristic was realized to within the ± 1 ns measurement uncertainty.

Introduction

IN RECENT YEARS much attention has been focused on the use of pulse compression in "Chirp" radar systems. Typical pulse compression filters used in these systems have bandwidths of a few megahertz or less and differential time delays of up to several hundred microseconds. Somewhat less attention has been given to the development of radar and receiver systems using microwave compression filters, one reason probably being that no satisfactory tehnique for designing and constructing compression filters with bandwidths of hundreds of megahertz existed.

The pulse compression filter is a device for decreasing the time duration of, or compressing, a frequency modulated pulse of RF energy. This compressed pulse is used to improve the resolution or scan-rate capability of systems which use an RF pulse to indicate some parameter to be measured.

The search for devices which could be used to make microwave pulse compression filters has led investigators to study a variety of techniques. These include the dispersive helix;[1] the tapped delay line with tuned taps;[2],[3] the tapped delay line with broadband untuned taps;[4] first- and second-order, allpass quaterwave coupled transmission lines;[5] the yttrium-iron-garnet delay line;[6] and the folded tape meander line (FTML).[7] The FTML was chosen as a desirable structure for implementing a large time-bandwidth product compression filter because of its relatively easily predictable performance, its compact size, and its comparatively low cost.

The Folded Tape Meander Line

Fig. 1 shows the physical configuration of the FTML and defines the dimensions used in equations to follow. The meander line is totally immersed in dielectric; this assumption is maintained throughout the text of this paper. In practice, this is quite easy to accomplish; two sheets of dielectric

Manuscript received May 17, 1967; revised July 24, 1967.

The anthor is with the Systems Techniques Laboratories, Stanford, Calif.